Dynamic histone H3 epigenome marking during the intraerythrocytic cycle of *Plasmodium falciparum*

Adriana M. Salcedo-Amaya[a], Marc A. van Driel[a], Blaise T. Alako[a], Morten B. Trelle[c], Antonia M. G. van den Elzen[a], Adrian M. Cohen[a], Eva M. Janssen-Megens[a], Marga van de Vegte-Bolmer[b], Rebecca R. Selzer[d], A. Leonardo Iniguez[d], Roland D. Green[d], Robert W. Sauerwein[b], Ole N. Jensen[c], and Hendrik G. Stunnenberg[a,1]

Departments of [a]Molecular Biology, Nijmegen Center for Molecular Life Sciences, Radboud University Nijmegen, and [b]Medical Microbiology, University Medical Center St. Radboud, 6500 HB, Nijmegen, The Netherlands; [c]Department of Biochemistry and Molecular Biology, University of Southern Denmark, DK-5230, Odense, Denmark; and [d]Roche-NimbleGen Inc., Madison, WI 53711

Edited by Jules A. Hoffmann, Centre National de la Recherche Scientifique, Strasbourg, France, and approved April 22, 2009 (received for review March 6, 2009)

Epigenome profiling has led to the paradigm that promoters of active genes are decorated with H3K4me3 and H3K9ac marks. To explore the epigenome of *Plasmodium falciparum* asexual stages, we performed MS analysis of histone modifications and found a general preponderance of H3/H4 acetylation and H3K4me3. ChIP-on-chip profiling of H3, H3K4me3, H3K9me3, and H3K9ac from asynchronous parasites revealed an extensively euchromatic epigenome with heterochromatin restricted to variant surface antigen gene families (VSA) and a number of genes hitherto unlinked to VSA. Remarkably, the vast majority of the genome shows an unexpected pattern of enrichment of H3K4me3 and H3K9ac. Analysis of synchronized parasites revealed significant developmental stage specificity of the epigenome. In rings, H3K4me3 and H3K9ac are homogenous across the genes marking active and inactive genes equally, whereas in schizonts, they are enriched at the 5′ end of active genes. This study reveals an unforeseen and unique plasticity in the use of the epigenetic marks and implies the presence of distinct epigenetic pathways in gene silencing/activation throughout the erythrocytic cycle.

chromatin | epigenetics | malaria

Plasmodium falciparum, the protozoan parasite causing malaria, exhibits a complex life cycle characterized by invasion of different cell types and hosts. During the ≈48 h of the intraerythrocytic cycle, a merozoite invades a red blood cell (RBC) and develops into the ring stage, which is followed by the trophozoite stage. Nuclear division marks the beginning of the schizont stage, which results in the formation of up to 32 merozoites that can invade new RBCs (1). Global analysis of transcription (2, 3) and protein expression (4, 5) of the parasite have revealed a high level of coordination in gene expression during the different stages of the life cycle. The absence of chromosomal clustering among genes with similar transitory expression profiles indicates that genes are regulated individually. The organization of *Plasmodium* spp. promoters is rather ill defined, and only a few DNA-binding proteins are known to control transcription (6–8). *Plasmodium* spp. genomes encode epigenetic modifiers such as histone acetyltransferases (HATs), deacetylases (HDACs), and methyltransferases (HMTs) (9, 10). Studies from yeast to humans have shown a strong correlation among active promoters and H3K4me3 and H3K9ac (11–15). However, recent studies challenge this notion by showing the occurrence of H3K4me3 at the promoter of inactive genes (16). In turn, H3K9me, H3K27me and H4K20me mark inactive genes and are involved in heterochromatin formation (17). In *P. falciparum*, epigenetic mechanisms have been implicated in the control of antigenic variation, a mechanism of immune evasion that contributes to pathogenicity (18–24). H3K9me3 has been described as the silenced *var* gene mark in targeted ChIP (18, 22) and H3K4me2–3 and H3K9ac as the active *var* gene marks (22). At other genomic locations, Cui et al. (25) analyzed H3K9me3 and H3K9ac and reported that acetylation is enriched at active stage-specific genes in the parasite (25). Comprehensive characterizations of the histone posttranslational modifications (PTMs) and full-genome epilandscaping of histone PTMs are lacking.

Here, we determined histone PTMs by MS in asexual stages and profiled their localization patterns using high-resolution microarray analysis. We identified an extensively euchromatic *P. falciparum* epigenome with limited and well defined heterochromatic islands. The vast majority of the genome displayed patterns of H3K4me3 and H3K9ac enrichment upstream but also downstream of genes. Analysis of synchronous ring and schizont parasites revealed a dynamic epigenome wherein H3K4me3 and H3K9ac are spread evenly across active and inactive genes in the ring stage and associate distinctively with the 5′ end of active genes at the postreplicative stage. The findings here suggest that H3K4me3 and H3K9ac are cycle-regulated at *P. falciparum* genes and challenge the notion that these marks are solely reflective of the transcriptional status in the parasite.

Results

We set out to study the epigenetic makeup and the role of histone PTMs in gene regulation. Acid-extracted histones from heterogeneous and highly purified parasites from infected RBC (iRBC) were subjected to Western blot analysis and high-accuracy MS analysis (for a detailed MS analysis of histone PTMs, see ref. 26). These analyses showed that *P. falciparum* H3 and H4 are extremely rich in euchromatin-associated PTMs and largely devoid of heterochromatin-associated marks (Fig. S1), as observed in other unicellular eukaryotes (27).

H3, H3K4me3, H3K9ac, and H3K9me3 Genomic Profiles. Posttranslational modification of histones and changes in chromatin structure are involved in establishment and maintenance of the expression status of genes. To gain insight into epigenetic control of gene expression in *P. falciparum*, we performed ChIP and ChIP-on-chip analyses during the intraerythrocytic cycle using antibodies that recognize H3 core, H3K4me3, H3K9me3, and H3K9ac. Assays were performed on cross-linked sonicated chromatin (XChIP) (H3, H3K4me3, and H3K9ac) or native chromatin (NChIP) (H3K9me3) obtained from cultures of asynchronous asexual parasites (50%

Author contributions: A.M.S.-A., M.B.T., O.N.J., and H.G.S. designed research; A.M.S.-A., M.B.T., A.M.G.v.d.E., A.M.C., E.M.J.-M., M.v.d.V.-B., R.R.S., and A.L.I. performed research; R.D.G., R.W.S., O.N.J., and H.G.S. contributed new reagents/analytic tools; A.M.S.-A., M.A.v.D., B.T.A., M.B.T., A.M.G.v.d.E., A.M.C., O.N.J., and H.G.S. analyzed data; and A.M.S.-A. and H.G.S. wrote the paper.

The authors declare no conflict of interest.

This article is a PNAS Direct Submission.

Data deposition: The data discussed in this publication have been deposited in NCBI's Gene Expression Omnibus and are accessible through GEO Series accession number GSE16096 (http://www.ncbi.nlm.nih.gov/geo/query/acc.cgi?acc=GSE16096).

[1]To whom correspondence should be addressed. E-mail: h.stunnenberg@ncmls.ru.nl.

This article contains supporting information online at www.pnas.org/cgi/content/full/0902515106/DCSupplemental.

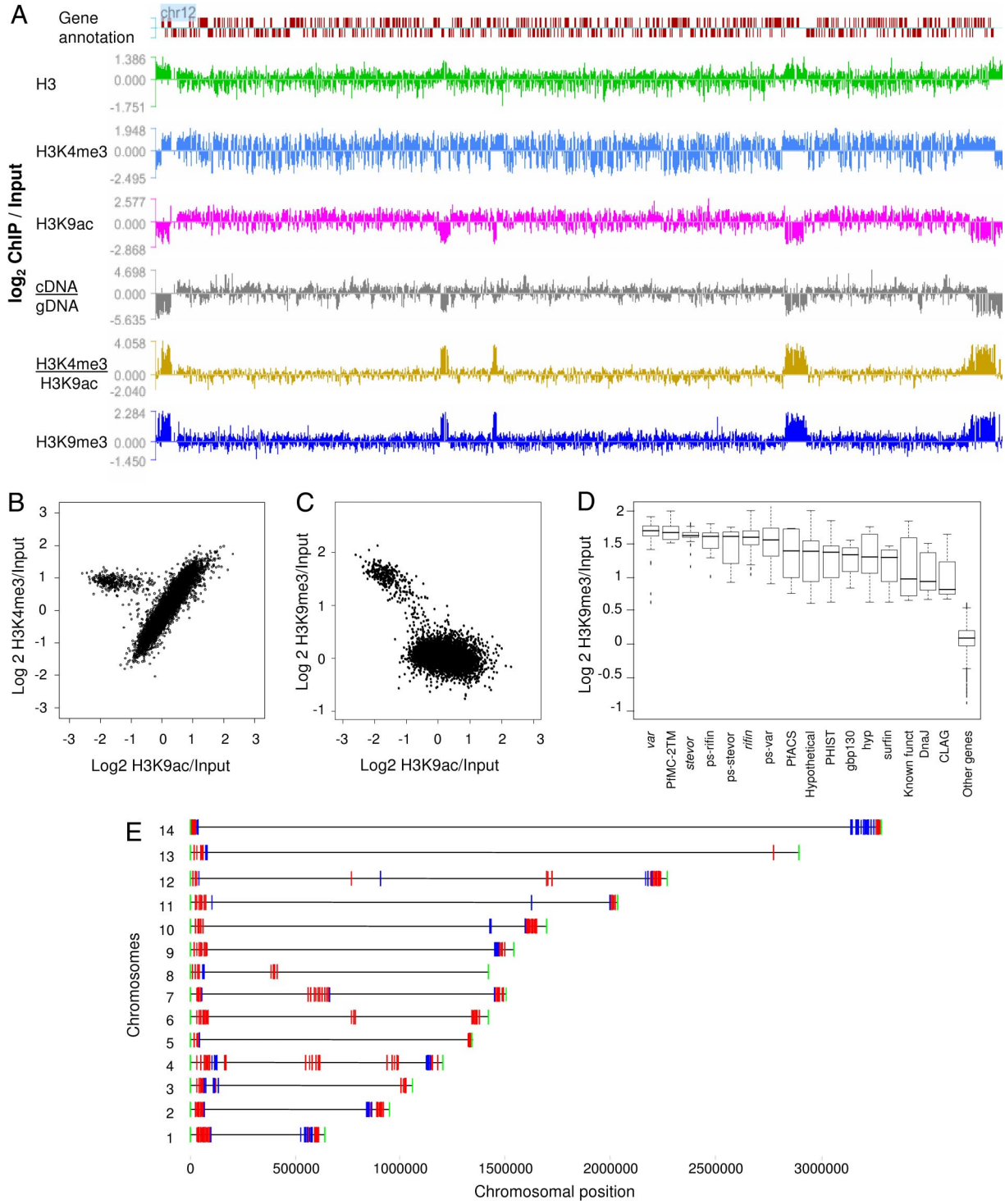

Fig. 1. Profiling H3, H3K4me3, H3K9ac and H3K9me3. (*A*) ChIP-on-chip and transcriptome profiles. SignalMap view of the epigenetic landscape of chromosome 12. The data are plotted as log2 ratios of ChIP/input. Coordinates are according to GenBank annotation release May 2005. (*B*) Scatter plot of log2 ratios (ChIP/input) of H3K9ac versus H3K4me3. Each dot represents the median ratio calculated per gene. (*C*) As in *B* for H3K9ac vs. H3K9me3. (*D*) Boxplot distribution of genes grouped according to gene annotation and ranked by their log2 H3K9me3 median ratio calculated per gene. (*E*) Genomic localization of hypoacetylated/hypermethylated genes. The chromosomal map positions of hypoacetylated 'outlier' genes. In red: *var*, *rifin*, *stevor*, and *pfmc-2tm* genes and their pseudogenes. In blue: Other known-function and hypothetical protein genes that show a similar hypoacetylation/hypermethylation described in the text and Table S1.

ring, 50% trophozoites-schizont). In addition, we collected and mined cDNA expression data (iRBC stages) on the microarray. To investigate the extent to which *P. falciparum* fragmented DNA can be reliably amplified, we tested 3 different amplification methods used in ChIP-on-chip studies. An optimized terminal transferase T7 amplification method (28) amplified the highly AT-rich DNA in the most reproducible and near-linear fashion (Fig. S2). A representative chromosomal view of the *P. falciparum* ChIP-on-chip land-

scape is shown in Fig. 1*A*. Histone H3 displays a rather even distribution throughout the genome with minor enrichment at telomeric and other regions. The general distribution pattern of H3K4me3 that we observe in *P. falciparum* is remarkable, because the modification does not appear to be restricted to specific regions, as in other eukaryotes, but rather enriched in a large fraction of the genome. H3K9ac yields a pattern that resembles the H3K4me3 pattern. Strikingly, extensively hypoacetylated transcriptionally silent regions are present at telomeric and discrete chromosome internal loci (Fig. 1*A*). Plotting ChIP/input ratios of H3K4me3 against H3K9ac at the single-probe level and at the mean value computed per ORF revealed a high correlation of H3K4me3 with H3K9ac for most of the *P. falciparum* genome, with the exception of a group of outliers that is strongly hypoacetylated but displays normal H3K4me3 (Fig. 1*B*).

H3K9me3-Heterochromatin Is Restricted to Subtelomeric and Discrete Interspersed Intrachromosomal Islands. We detected very low levels of H3K9me3 in our MS analysis and could not unambiguously determine its presence by XChIP because of poor recoveries and signal-to-noise ratios. We reasoned that H3K9me3 may be shielded by chromatin-associated proteins in XChIP. Therefore, we have established a modified native ChIP (NChIP) protocol, which in our hands considerably improves the efficiency and accuracy of the ChIP analysis for H3K9me3. At *var* genes, we observe a 6-fold enrichment of H3K9me3 when compared with the active *hsp70* gene and a near-perfect inverse correlation with H3K9ac (Fig. S3). NChIP-on-chip analysis of H3K9me3 showed that this PTM is common to all H3K9ac hypoacetylated, silent "outlier" genes (Fig. 1*A*), with a strong anticorrelation between H3K9ac and H3K9me3 (Fig. 1*C*). The H3K9 hypoacetylated and hypertrimethylated regions are located either close to telomeres or in intrachromosomal clusters (Fig. 1*E*). These regions comprise nearly all members of variant surface antigen families (VSA), *var*, *rifin*, *stevor*, and *pfmc-2tm*, and other subtelomeric gene families such as *pfacs*, *surfins*, *clag*, and many members of exported proteins families such as *hyp*, *dnaj*, *gbp130*, and *phist* genes. Thirty-five hypothetical proteins and 12 known function proteins that are hitherto not linked in any way to VSA genes also share this marking (Fig. 1*D* and Table S1). These genes are flanked by or adjacent to antigenic variation genes (Fig. 1*E*), with the exception of a small number of isolated single genes (i.e., chromosomes 10, 11, and 12 shown in Fig. 1*E*). Interestingly, 27 of these 35 hypothetical proteins are *P. falciparum*-specific and not conserved in any of the other sequenced *Plasmodium* species.

var genes are implicated in host–parasite interactions and pathogenicity and are subject to mutually exclusive expression: only 1 *var* gene is active in individual parasites (29, 30). Although several *var* genes may be active in different subsets of the parasites, in our cultures, they are on average silent, as corroborated by expression profiling (Fig. 1*A*). Silent *var* genes have been reported to be trimethylated on H3K9 (18, 22). qPCR validation and our positional map for the average silent *var* gene corroborate and extend that H3K9me3 and H3K4me3 are elevated over these genes (Fig. S3). In contrast, H3K9ac is strongly depleted at the *var* genes.

H3K4me3 and H3K9ac Are Highly Correlated and Enriched at Intergenic Regions and Depleted at the Majority of Genes in *P. falciparum*. In all organisms studied thus far, H3K4me3 and H3K9ac localize with active or poised promoters providing positional and probably also functional information for gene expression (11–15, 31). During RBC infection, at least 60% of all *P. falciparum* genes are found expressed in a highly coordinated manner in which functionally similar groups of transcripts are produced when needed during the RBC cycle (2, 3). Zooming into the mixed asexual parasites profiles to the gene level, core histone H3 displayed minimal patterns of enrichment that correlate with ORFs (Fig. 2*A*). In contrast, H3K4me3 and H3K9ac display clear patterns that correlate well

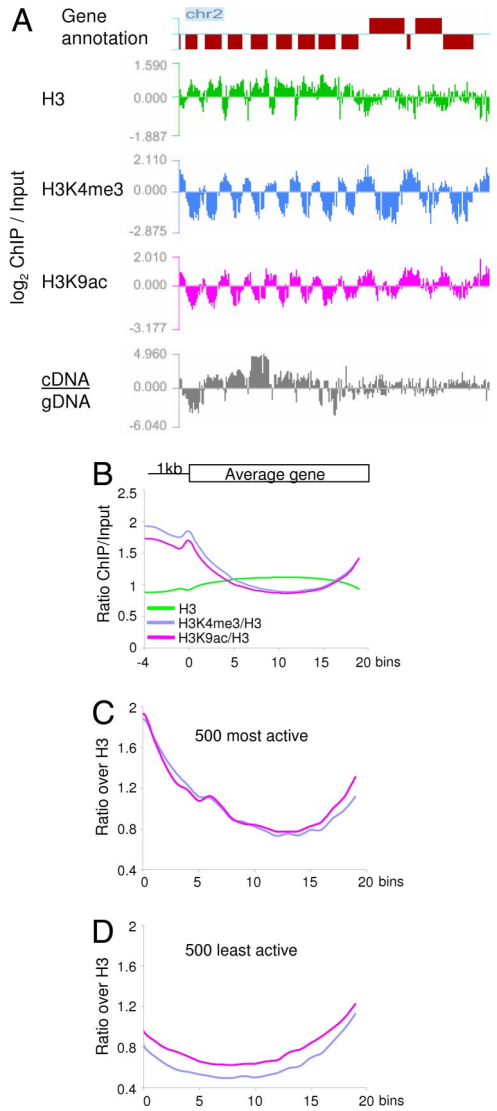

Fig. 2. H3K4me3 and H3K9ac analysis in asexual RBC stages. (*A*) SignalMap view of a section of chromosome 2 as described in Fig. 2*A* showing increased marking at intergenic regions and depletion at ORFs. (*B*) Composite epigenetic profiles of H3, H3K4me3, and H3K9ac averaged over *P. falciparum* genes. The averaged gene organization is depicted. Only genes with gene-free upstream region larger than 0.8 kb and >4 probes spanning it were analyzed. Probes located within 0.8 kb upstream of the ORF were assigned into 5 bins of equal length. ORFs were divided into 20 bins. The middle position of the probe was used to assign probes to bins. (*C*) Composite profile of H3K4me3/H3 and H3K9ac/H3 ratios of the 500 highest expressed genes in iRBCs. Each ORF was divided into 20 bins of equal size. Genes larger than 0.8 kb with upstream gene-free region larger than 0.8 kb were used for the analysis. (*D*) As in *C* for the 500 least expressed genes.

with the gene annotation, i.e., high at intergenic regions (IGRs) and low at ORFs (Fig. 2*A*). This pattern, best discernable at large ORFs, is characterized by high signals upstream of the ORF, which decrease within the gene and increase again toward the 3′ end, as shown by the computed averaged modification profiles over all ORFs (Fig. 2*B*). ChIP-qPCR experiments using primers ≈1 kb upstream from the ORF and within the gene bodies of transcriptionally active and inactive genes validate this finding (Fig. S4). Remarkably, the ChIP recoveries are similar between active and inactive genes in terms of H3, H3K4me3, and H3K9ac. For example, the mosquito stage-specific genes, *ssp2* and *csp*, whose transcript levels are very low to undetectable in iRBC stages, are

acetylated and methylated to an extent and in a pattern similar to those of the highly transcribed *hsp70* and *hsp 86* genes (Fig. S4). Analysis by re-ChIP, carrier ChIP-like approaches, and NChIP showed the same results at these genomic regions (Fig. S5).

To further investigate the relationship between gene expression and histone modifications, we compared the marking of the 500 most active genes in iRBCs with that of the 500 most inactive genes extracted on the basis of our expression study and excluding the "outlier" group. The calculated average profiles revealed that H3K4me3 and H3K9ac extend into the 5′ region of the highest expressed genes, gradually decreasing toward the middle of the gene and increasing back again toward the 3′ end (Fig. 2*C*). Interestingly, the lowest expressed genes display lower H3K4me3 and H3K9ac at the beginning of the gene (Fig. 2*D*). The particular enrichment of H3K9ac and H3K4me3 at the 5′ end of active genes is suggestive of promoter-specific marking by relative enrichment as observed in the closely related *Toxoplasma gondii* (32).

H3K4me3 and H3K9ac Gene Patterns Are Dynamically Regulated Throughout the *P. falciparum* iRBC Cycle. To further assess the role of histone PTMs in relation to gene expression, we set out to analyze genes that are constitutively in/active and genes that change expression throughout the iRBC cycle. RNA and chromatin were collected from ring parasites 14–18 h postinvasion and from mature schizonts ≈4 h preegression. Expression analysis and ChIP and ChIP-on-chip experiments were carried out in parallel. Reverse transcriptase-PCR shows that our ring parasites indeed displayed high mRNA levels of the ring-specific marker *kahrp*, whereas the schizont sample contains high levels of *msp2* and *actin* (Fig. S6). Global gene expression analyzed on the same microarray corroborates and extends that the 2 populations display differential gene expression (Fig. S6) (2, 3).

Next, we examined the epigenetic marking over the 500 highest and least expressed genes in rings (prereplication) and mature schizonts (postreplication). In rings, the marks are evenly distributed across the genes with a minor increase over active as compared with inactive genes (Fig. 3 *A* and *B*). Remarkably, the profile in schizonts differs significantly from that in rings. H3K4me3 and H3K9ac are found specifically enriched toward the 5′ end of highly active genes (Fig. 3*C*), similar to the small increase observed in the asynchronous mixed stages (Fig. 2*C*). Genes inactive in schizonts lack this 5′ end marking but display a slight enrichment of the histone marks toward the 3′ end (Fig. 3*D*), as also observed in the analysis of the mixed population (Fig, 2*D*). This H3K4me3 and H3K9ac enrichment at the 5′ end of active genes in schizonts was confirmed by qPCR analysis of constitutive active and inactive genes as shown in Fig. S7.

Given the important differences in the marking between ring and schizont stages, we analyzed the expression and histone marks of the genes that are differentially or constitutively expressed in rings and schizonts. For clarity, only genes belonging to the top (active) and bottom quartiles (inactive) of gene expression are included in the analysis. Genes active in ring (Fig. 3*A*) that remain very active as the cycle progresses into the schizont stage (223/500) gain elevated H3K4me3 and H3K9ac at the 5′end characteristic of active genes in the schizont stage of the parasite cycle (Fig. 3*E*). Genes active in rings and switched off in schizonts display a nearly flat level at the 5′ end (49 genes) (Fig. 3*F*). Inactive ring genes (Fig. 3*B*) that become highly expressed in schizonts (86 genes) also display enrichment of H3K4me3 and H3K9ac at their 5′ end (Fig. 3*G*). Importantly, genes that are inactive in rings and that remain inactive in schizonts (291) lack enrichment of the marks at their 5′ end (Fig. 3*H*). Following the fate of the 500 most active schizont genes (Fig. 3*C*) into the ring stage reveals loss of the distinct marking at the 5′ end. The PTMs are found almost evenly distributed along the length of the gene with very little differences in the profile between active (225 genes) (Fig. 3*I*) and silent genes (140 genes) (Fig. 3*J*). Likewise, inactive schizont genes that became strongly activated in

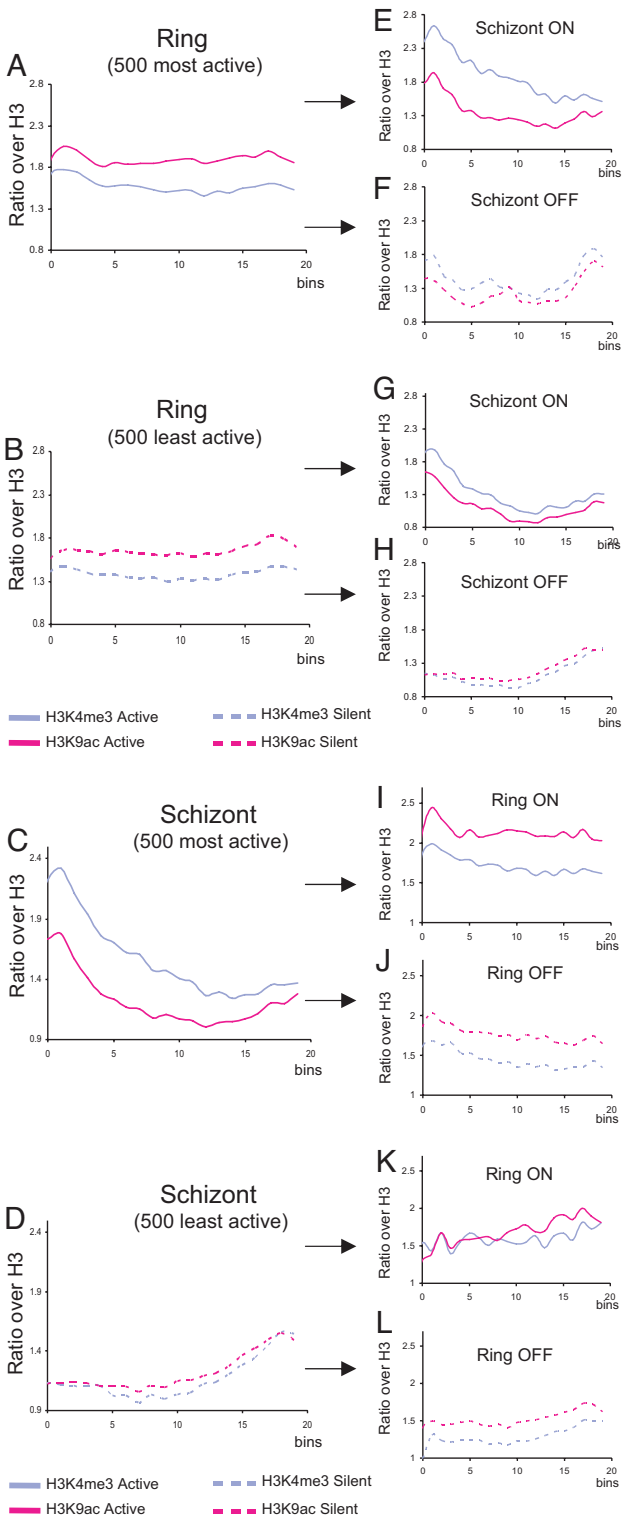

Fig. 3. Distinct epigenetic marking of genes in the ring and schizont stages. (*A*) Composite profiles of H3K4me3/H3 and H3K9ac/H3 ratios of the 500 most active genes in rings. Each ORF was divided into 20 bins of equal size. Only genes larger than 0.8 kb with upstream gene-free region larger than 0.8 kb were taken for the analysis. (*B*) The 500 least-active genes in rings; (*C*) 500 most-active genes in schizonts; (*D*) 500 least active genes in schizonts. (*E*) Schizonts profile of genes that are active in rings and remain active in schizonts, and of *F*, genes that are active in rings and turn inactive in schizonts. (*G*) Schizont profile of genes that are inactive in rings and became active in schizonts and of *H*, genes that are inactive in rings and remain inactive in schizonts. (*I* and *J*) Ring profiles of genes as they switch from schizonts to rings, as described from *E*–*H*.

the ring stage (46 genes) (Fig. 3*K*) or that remained inactive (387) (Fig. 3*L*) are marked in the ring stage seemingly independent of their gene expression level. Thus, gene expression in rings does not correlate to a specific pattern of H3K4me3 and H3K9ac such as is found at the schizont stage. The specification of active genes by H3K4me3 and H3K9ac at the 5′ end in the schizont stage is lost at the ring stage, where these marks spread evenly across the genes. These findings suggest that the *P. falciparum* epigenome is unique, highly dynamic, and stage-specific.

Discussion

To decipher the epigenetic component of gene regulation, we first identified histone PTMs and subsequently analyzed their distribution genome-wide in mixed asexual stages. The characterization of H3 and H4 PTMs by Western blot analysis and MS (Fig. S1) supports the conclusion that *P. falciparum* histones are highly enriched in euchromatin-associated histone PTMs and low in heterochromatin marks, as seen with other unicellular eukaryotes (27).

Our epigenome profiling of histone H3 marks reveals a restricted epigenetic marking characterized by hypoacetylation and hypertrimethylation of H3K9 over ≈9% of the parasite genome that encompasses VSA genes, exported proteins, and other hitherto unrelated genes. H3K9me3 marking has been reported before on individual *var* genes (18, 22). Our genome-wide findings are in good agreement with a very recently published study reporting the localization of H3K9me3 (24). Both studies have been conducted using a NimbleGen platform with different array designs. Due to low sequence complexity and a high AT content, neither of the 2 arrays has sufficient probes and hence discriminatory power in the IGRs. Therefore, we restricted our comparative analysis of the 2 H3K9me3 datasets to the ORFs, which revealed largely identical gene lists. We obtained high recoveries of H3K9me3 only when using NChIP, indicating that a protein(s) may be tightly associated with H3K9me3, which upon cross-linking masks the mark. In higher eukaryotes, H3K9me3 is a hallmark of heterochromatin and recruits HP1; recent data have shown that a chromodomain protein related to HP1 also recognizes this mark in *P. falciparum* (33).

H3K4me3 and H3K9ac have been correlated to the active *var* gene state (22). It is important to note that our study cannot be compared directly to the active *var2csa* gene study (22), because we used parasites in which *var* expression is not characterized. Moreover, due to the repetitiveness of the *var* upstream regions, our analysis lacks the power to discriminate among individual promoters. We provide evidence that the average silent *var* gene is decorated with H3K9me3, whereas H3K9ac is low (Figs. 1 and S3). Contrasting with the findings of Lopez-Rubio et al. (22), loci with high H3K9me3 also display high H3K4me3. We cannot at present exclude that the presence of these opposing marks is due to variegated expression in unselected parasite populations. How the highly localized and well delineated hypermethylated/hypoacetylated islands (Fig. 1) are generated and insulated may be the subject of future investigations. Interestingly, only 8 genes with this distinctive heterochromatic makeup are conserved in all sequenced *Plasmodium* spp. H3K9me3 does not appear to be present at other *P. falciparum* inactive genes outside of the heterochromatic blocks. For instance, H3K9me3 is not detectable at transcriptionally inactive genes such as the *csp* and *ssp2* genes, indicating that H3K9me3 is not a general mark of transcriptional inactivity in the parasite. Other layers of transcriptional repression may be involved in the silencing of blood stage-specific genes and genes expressed at other stages of the parasite cycle. In our MS analysis, we detect K9me3 along with the replication-linked K56ac exclusively on H3 and not H3.3. Extending from studies in yeast (34, 35), we speculate that the acquisition of H3K56ac occurs during or soon after DNA replication.

Our study uncovers a predominantly euchromatic *P. falciparum* epigenome characterized by high overall levels of H3K4me3 and H3K9ac, generally enriched over IGRs and lower at ORFs in mixed asynchronous parasite cultures. This euchromatic marking extends to 91% of the genome (Fig. 2). In yeast, H3K4me and histone acetylation are positively correlated with transcription and are found to be enriched not only at the promoter but also at the 5′ end of the coding regions of transcribed genes (13, 14, 36). Analyses of the IGRs in *P. falciparum* did not reveal convincing differences between active and inactive genes by either ChIP-qPCR or microarray analysis in nonsynchronized cultures. Analysis of synchronized stages reveals that at the ring stage, the PTMs are distributed rather homogenously along the length of the gene. Genes most highly expressed in the ring stage display only marginally higher H3K4me3 and H3K9ac as compared with genes that are lowest or not transcriptional active (Fig. 3 *A*, *B*,and *I*--*L*). Thus, the extent of H3K4me3 and H3K9ac does not appear to correlate with transcription in the ring stage of the parasite. This occurrence of active marks on inactive genes is unexpected and contrary to the currently held view that gene activity correlates with the presence of H3K4me3 and H3K9ac at promoters.

Unlike in the ring stage, active genes in schizonts are enriched for H3K4me3 and H3K9ac specifically at the 5′ end of ORFs (Fig. 3 *C*, *E*, and *G*), whereas inactive genes lack this marking (Fig. 3 *D*, *F*, and *H*). This H3K4me3 and H3K9ac marking is acquired primarily in a stage- rather than a gene-specific manner. In rings, ring-specific, constitutively active but also inactive genes (Fig. 3 *I*–*L*) display a similar evenly spread profile over the gene. In schizonts, constitutively expressed (Fig. 3 *E* and *H*) and schizont-specific genes (Fig. 3 *F* and *G*) display elevated levels of H3K4me3 and H3K9ac at their 5′ ends, reminiscent of active promoters in other eukaryotes (11–15).

Previous studies of gene regulation in *P. falciparum* have supported the view that epigenetic modifications and chromatin changes are critical players in the control of gene expression (37). In this study, we report the existence of distinct stage-specific epigenetic marking of genes in the parasite, indicating that the epigenome is dynamically regulated during the parasite blood cell cycle. The distinctive marking of genes in rings and schizonts might be the result of differential availability of the components of the epigenetic machinery at different stages of the parasite cycle. The similarity between the profiles of genes active in yeast and genes active in the schizont stage is striking, suggesting that temporarily expressed modifiers may be shaping the profiles postreplication. The histone deacetylase containing Rpd3S complex in yeast has been involved in removing transcription-related acetylation toward the 3′ end of active genes (39). Whether a related complex is present in *P. falciparum* specifically in the postreplicative stage of the life cycle remains to be investigated. Our discovery of the lack of association of H3K4me3 and H3K9ac with gene expression in the ring stage supports a model of concerted integration of different levels of control (10, 38).

Taken together, the striking differences in the marking of genes in the ring and schizont stages uncovers that the process of epigenome marking is dynamic and changes throughout the course of RBC infection. The challenge that lies ahead is to generate quantitative transcriptome and epigenetic maps at mononucleosomal resolution throughout all stages of the RBC life cycle. These detailed maps may be instrumental in understanding parasite growth, control of gene expression, in particular of pathogenicity genes, and disease development. Excitingly, given the observed differences in the epigenetic code compared with all other organisms studied, including humans, this knowledge will open new avenues for therapeutic interference using *Plasmodium*-specific epigenetic enzymes inhibitors.

Materials and Methods

Parasites Preparation. *P. falciparum* NF54 was cultured using a semiautomated culture system. Mixtures of asexual parasites contained ≈10% ring parasitemia and 10% trophozoite-schizont parasitemia. For MS, parasites were

filtered to remove white blood cells (WBC) and further purified using the VarioMacs system. Synchronous asexual cultures were obtained by sequential use of at least 2 rounds of 5% Sorbitol and 63% Percoll. Rings were collected ≈14–18 h postinfection and mature schizonts ≈4 h pre-egress. Parasites were released from erythrocytes by treatment with saponin 0.06% or RBC Lysing Buffer Hybri-Max (Sigma–Aldrich).

Antisera. H3 (Abcam ab1791), H3K4me2 (Abcam 7766), H3K4me3 (Abcam ab8580), H3K9ac (Upstate 06942), H3ac (Upstate 06–599), H3K9me3 [#4861; (40)], H3R17me2 (Abcam ab8284), H3K18ac (Abcam ab1191), H4ac (Upstate 17–211), H4K8ac (Upstate 06–760), H4K12ac (Upstate 06–761), H4K20me1 and H4K20me3 (41).

Chromatin Immunoprecipitation. Cross-linked and native chromatin were prepared as described in *SI Methods*.

Microarray Analyses. A microarray was designed for whole-genome analysis based on the *P. falciparum* National Center for Biotechnology Information genomic sequence (May 2005) with a mean probe spacing of 47 bp. The procedure for oligo selection is described in *SI Methods*. For ChIP-on-chip hybridization, total and ChIP DNA were amplified starting from similarly low DNA concentrations using T7 Linear Amplification method (28). We used G tailing instead of T tailing and a T7C9B primer. Three to five micrograms of amplified RNA were reverse-transcribed using N6 primers. Double-strand DNA was synthesized according to enzyme manufacturer protocols. Labeling of dsDNA was performed using 5′-Cy3 or Cy5 labeled random heptamers (TriLink Biotechnologies). For transcriptional profiling of iRBC stages, cDNA obtained from RNA (*SI Methods*) and sonicated genomic DNA (obtained from early rings) were directly labeled with random heptamers and hybridized.

Data Analysis. Log2 ratios were computed for each sample pair and adjusted using Tukey biweight (affy-package version 1.6.7, Bioconductor). General feature format (GFF) tracks were visualized using SignalMap (NimbleGen Inc.). Data presented for asynchronous asexual stages are the mean of: H3 (4), H3K4me3 (2), H3K9ac (3), cDNA (1), and H3K9me (1) biological replicas. For synchronized ring and schizont stages, each factor was done once. Average gene plots were generated based on the gene annotation of National Center for Biotechnology Information's Gene database (Sequence release May 2005). Only genes covered by >5 probes were included. For the resulting 5,266 genes, we calculated the average H3, H3K4me3, H3K9ac, and H3K4me3 to H3K9ac plots and ratio values. For detection of H3K9me3 enriched genes, genes covered by >2 probes were included. Outliers with H3K9me3 deviating from the genome average were defined as those with values >3 times the interquantile range and grouped according to gene name and/or function. Genes in the outlier group were rank-ordered according to the median H3K9me3 ratios.

For transcriptional analysis, the expression value per gene was calculated by averaging the cDNA/gDNA non-log ratio of all of the probes mapping to the exons of the gene.

ACKNOWLEDGMENTS. We thank our colleagues at the Department of Molecular Biology for discussion and critical reading of the manuscript. This work was supported by The Netherlands Organization for Scientific Research (NWO-CW-TOP 700.53.311 and NWO-Genomics 050-10-053) and the European Commission (BioMalPar LSHP-CT-2004-503578). O.N.J. was supported by the Danish Agency for Science, Technology and Innovation and the Lundbeck Foundation.

1. Arnot DE, Gull K (1998) The *Plasmodium* cell-cycle: Facts and questions. *Ann Trop Med Parasitol* 92:361–365.
2. Bozdech Z, et al. (2003) The transcriptome of the intraerythrocytic developmental cycle of *Plasmodium falciparum*. *PLoS Biol* 1:E5.
3. Le Roch KG, et al. (2003) Discovery of gene function by expression profiling of the malaria parasite life cycle. *Science* 301:1503–1508.
4. Florens L, et al. (2002) A proteomic view of the *Plasmodium falciparum* life cycle. *Nature* 419:520–526.
5. Lasonder E, et al. (2002) Analysis of the *Plasmodium falciparum* proteome by high-accuracy mass spectrometry. *Nature* 419:537–542.
6. Coulson RM, Hall N, Ouzounis CA (2004) Comparative genomics of transcriptional control in the human malaria parasite *Plasmodium falciparum*. *Genome Res* 14:1548–1554.
7. De Silva EK, et al. (2008) Specific DNA-binding by apicomplexan AP2 transcription factors. *Proc Natl Acad Sci USA* 105:8393–8398.
8. Gardner MJ, et al. (2002) Genome sequence of the human malaria parasite Plasmodium falciparum. *Nature* 419:498–511.
9. Aravind L, Iyer LM, Wellems TE, Miller LH (2003) *Plasmodium* biology: Genomic gleanings. *Cell* 115:771–785.
10. Horrocks P, Wong E, Russell K, Emes RD (2009) Control of gene expression in *Plasmodium falciparum*--Ten years on. *Mol Biochem Parasitol* 164:9–25.
11. Schubeler D, et al. (2004) The histone modification pattern of active genes revealed through genome-wide chromatin analysis of a higher eukaryote. *Genes Dev* 18:1263–1271.
12. Schneider R, et al. (2004) Histone H3 lysine 4 methylation patterns in higher eukaryotic genes. *Nat Cell Biol* 6:73–77.
13. Pokholok DK, et al. (2005) Genome-wide map of nucleosome acetylation and methylation in yeast. *Cell* 122:517–527.
14. Liu CL, et al. (2005) Single-nucleosome mapping of histone modifications in *S. cerevisiae*. *PLoS Biol* 3:e328.
15. Bernstein BE, et al. (2005) Genomic maps and comparative analysis of histone modifications in human and mouse. *Cell* 120:169–181.
16. Guenther MG, Levine SS, Boyer LA, Jaenisch R, Young RA (2007) A chromatin landmark and transcription initiation at most promoters in human cells. *Cell* 130:77–88.
17. Martens JH, et al. (2005) The profile of repeat-associated histone lysine methylation states in the mouse epigenome. *EMBO J* 24:800–812.
18. Chookajorn T, et al. (2007) Epigenetic memory at malaria virulence genes. *Proc Natl Acad Sci USA* 104:899–902.
19. Duraisingh MT, et al. (2005) Heterochromatin silencing and locus repositioning linked to regulation of virulence genes in *Plasmodium falciparum*. *Cell* 121:13–24.
20. Frank M, et al. (2006) Strict pairing of var promoters and introns is required for var gene silencing in the malaria parasite *Plasmodium falciparum*. *J Biol Chem* 281:9942–9952.
21. Freitas-Junior LH, et al. (2005) Telomeric heterochromatin propagation and histone acetylation control mutually exclusive expression of antigenic variation genes in malaria parasites. *Cell* 121:25–36.
22. Lopez-Rubio JJ, et al. (2007) 5′ flanking region of var genes nucleate histone modification patterns linked to phenotypic inheritance of virulence traits in malaria parasites. *Mol Microbiol* 66:1296–1305.
23. Voss TS, et al. (2006) A var gene promoter controls allelic exclusion of virulence genes in *Plasmodium falciparum* malaria. *Nature* 439:1004–1008.
24. Lopez-Rubio JJ, Mancio-Silva L, Scherf A (2009) Genome-wide analysis of heterochromatin associates clonally variant gene regulation with perinuclear repressive centers in malaria parasites. *Cell Host Microbe* 5:179–190.
25. Cui L, et al. (2007) PfGCN5-mediated histone H3 acetylation plays a key role in gene expression in *Plasmodium falciparum*. *Eukaryot Cell* 6:1219–1227.
26. Trelle MB, Salcedo-Amaya AM, Cohen AM, Stunnenberg HG, Jensen ON (2007) Global histone analysis by mass spectrometry reveals a high content of acetylated lysine residues in the malaria parasite *Plasmodium falciparum*. *J Proteome Res*, in press.
27. Garcia BA, et al. (2007) Organismal differences in post-translational modifications in histones H3 and H4. *J Biol Chem* 282:7641–7655.
28. Liu CL, Schreiber SL, Bernstein BE (2003) Development and validation of a T7 based linear amplification for genomic DNA. *BMC Genomics* 4:19.
29. Horrocks P, Pinches R, Christodoulou Z, Kyes SA, Newbold CI (2004) Variable var transition rates underlie antigenic variation in malaria. *Proc Natl Acad Sci USA* 101:11129–11134.
30. Scherf A, et al. (1998) Antigenic variation in malaria: In situ switching, relaxed and mutually exclusive transcription of var genes during intra-erythrocytic development in *Plasmodium falciparum*. *EMBO J* 17:5418–5426.
31. Vermeulen M, et al. (2007) Selective anchoring of TFIID to nucleosomes by trimethylation of histone H3 lysine 4. *Cell* 131:58–69.
32. Gissot M, Kelly KA, Ajioka JW, Greally JM, Kim K (2007) Epigenomic modifications predict active promoters and gene structure in *Toxoplasma gondii*. *PLoS Pathog* 3:e77.
33. Perez-Toledo K, et al. (2009) *Plasmodium falciparum* heterochromatin protein 1 binds to tri-methylated histone 3 lysine 9 and is linked to mutually exclusive expression of var genes. *Nucleic Acids Res* 37:2596–2606.
34. Li Q, et al. (2008) Acetylation of histone H3 lysine 56 regulates replication-coupled nucleosome assembly. *Cell* 134:244–255.
35. Ozdemir A, Masumoto H, Fitzjohn P, Verreault A, Logie C (2006) Histone H3 lysine 56 acetylation: A new twist in the chromosome cycle. *Cell Cycle* 5:2602–2608.
36. Ng HH, Robert F, Young RA, Struhl K (2003) Targeted recruitment of Set1 histone methylase by elongating Pol II provides a localized mark and memory of recent transcriptional activity. *Mol Cell* 11:709–719.
37. Hakimi MA, Deitsch KW (2007) Epigenetics in Apicomplexa: Control of gene expression during cell cycle progression, differentiation and antigenic variation. *Curr Opin Microbiol* 10:357–362.
38. Coleman BI, Duraisingh MT (2008) Transcriptional control and gene silencing in *Plasmodium falciparum*. *Cell Microbiol* 10:1935–1946.
39. Carrozza MJ, et al. (2005) Histone H3 methylation by Set2 directs deacetylation of coding regions by Rpd3S to suppress spurious intragenic transcription. *Cell* 123:581–592.
40. Peters AH, et al. (2003) Partitioning and plasticity of repressive histone methylation states in mammalian chromatin. *Mol Cell* 12:1577–158942.
41. Schotta G, et al. (2004) A silencing pathway to induce H3–K9 and H4–K20 trimethylation at constitutive heterochromatin. *Genes Dev* 18:1251–1262.